Intermolecular Potential Calculations for Polynuclear Aromatic Hydrocarbon Clusters

Jennifer D. Herdman and J. Houston Miller*

Department of Chemistry, The George Washington University, Washington, District of Columbia 20052

Received: January 17, 2008; Revised Manuscript Received: April 23, 2008

Calculations of intermolecular potentials are presented for homo-molecular and hetero-molecular clusters of 24 peri-condensed PAH spanning monomer masses ranging from 78 to 1830 Da. Binding energies of homo-molecular dimers rise rapidly with molecular size and asymptotically approach the experimentally established exfoliation energy for graphite of 5.0 kJ mol^{-1} (carbon atom)$^{-1}$. Binding energies of hetero-molecular dimers correlate well with the reduced mass of the pair. From calculations of homo-molecular stacks, binding energies were observed to increase with each added molecule and rise asymptotically, approaching a limit which scales linearly with monomer molecular mass. These results are reviewed in the context of molecular growth in flames and in the context of astrophysical observations.

Introduction

Soot formation in hydrocarbon (HC) flames is kinetically controlled and occurs in short times (1−10 msec to reach particle diameters of 500 Å).[1] Polynuclear aromatic hydrocarbons (PAH) have often been invoked as important intermediates in this chemistry. These species, which are found in all sooting and HC flames, have structures similar to that of soot's graphitic morphology and posses C/H ratios between those of most starting fuels (<1) and soot particles (>5).

In several landmark papers in the mid 1980s, key kinetic and thermodynamic arguments were made that established the central role of condensed PAH systems in soot formation. Frenklach et al. developed a kinetic model for the high-temperature pyrolysis of acetylene in shock tubes.[2] In their mechanism, the initial chemistry forms unsaturated HC radicals that undergo cyclization to form benzene. Historically, it was thought that this process proceeded through a sequential addition of C_2 species (i.e., acetylene).[3] More recently, a consensus has developed that much of the benzene formation rate is carried through the combination of two resonantly stabilized propargyl radicals.[4–6] The ensuing formation of PAH rings from benzene is thought to occur as a hydrogen abstraction reaction followed by acetylene addition to the radical aromatic core (a scheme known by the abbreviation HACA).[3]

Soon after the original Frenklach et al.'s paper publication, Stein and Fahr evaluated the thermodynamic stabilities of HCs with the empirical formula $C_{2n}H_{2m}$ with *n* ranging from 1 to 21 and *m* from 1 to 8.[7] As noted by these authors, at or near 300 K, large HCs favor sp^3 bonding (such as that found in diamond). At very high temperatures (>3000 K), polyacetylenes are the most stable bonding configuration. In the intermediate temperature range, PAH become the thermodynamically stable HC form. Within this class, the number of isomers grows rapidly with molecular mass. Stein and Fahr found that near temperatures typical of molecular growth in flames, the most stable isomers were those with a central core of condensed, 6-membered aromatic rings.[7] Molecules along this path of stability have become known collectively as the stabilomer grid (Figure 1).

As a direct consequence of the wide acceptance of the ideas in these early papers, essentially all models for soot inception begin with the assumption that the early chemistry results in the formation of highly condensed aromatic structures. However, at some point in the molecular growth process, the magnitude of non-bonded interactions is large enough so that chemical bonding is no longer a requirement for sticking. For more than a decade, an active debate is occurring, aimed at defining this transition. Currently, many numerical simulations of soot formation in flames commonly invoke irreversible binding of molecules as small as pyrene,[8] despite the fact that there is no definitive experimental data to support the claim.

Non-bonded interactions between small molecules such as gas-phase fuels and their oxidation products produce attractive wells that are shallow (≲2 kJ/mol) compared to the average kinetic energy available in molecular collisions ($k_BT \approx 10-12$ kJ/mol in rich regions of flames) and chemical bonds (∼400 kJ/mol) and are thus thermally inconsequential in flames. However, the attractive interactions between π electrons in aromatic systems are among the strongest non-covalent interactions in nature and govern binding in systems ranging from biomolecular recognition in DNA and proteins to macrocyclic molecular wires.[9] In graphite, adjacent sheets are bound by a well of ∼5.0 kJ/mol per carbon atom.[10] Thus, two graphene sheets of 100 carbon atoms each would be bound more tightly than a typical covalent, carbon−carbon single bond.

As noted above, over the past twenty years, other researchers and we have hypothesized that PAH agglomeration in flames occurs at modest molecular size.[11–13] To investigate this hypothesis, equilibrium concentrations for PAH dimers in flames have been calculated using estimated monomer concentrations and dimerization equilibrium constants calculated from model dispersive and electrostatic potentials.[14] Because dimer concentrations were less than the number densities of the earliest soot particles, homogeneous nucleation of PAH was deemed less important than chemical growth in particle inception. A potential flaw in this analysis may have been the assumption of equilibrium in the dimerization steps. Several years later, the problem was revisited from a kinetic perspective. In this later analysis, the lifetimes of dimers under flame conditions were calculated by assuming that the energy of the initial collision could be either accommodated by the PAH molecules themselves or removed by molecules in the bath. Our hypothesis was that PAH agglomeration would contribute to particle growth

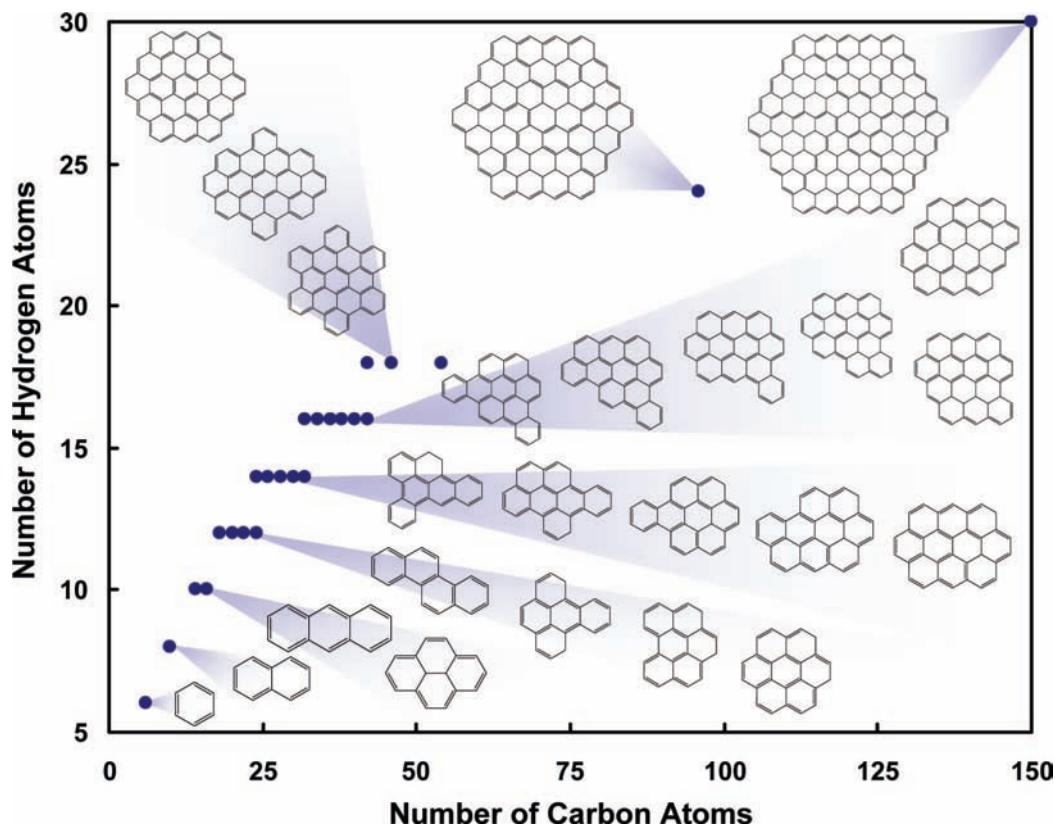* Corresponding author. E-mail: houston@gwu.edu.

Figure 1. PAH extracted from Stein and Fahr's stabilomer grid[94] that were implemented in this study.

if the dimer lifetimes were long with respect to the characteristic time for chemical growth. Our conclusion at the time was that this process could occur but only for relatively large PAH species (>800 Da). However, our calculation of energy accommodation during collision neglected conversion of the collisional kinetic energy into internal molecular degrees of freedom. More recently, Schuetz and Frenklach used a molecular dynamics approach using semi-empirical force fields to calculate dimer lifetimes for pyrene under flame conditions.[15] They found that deposition of energy into internal rotations in the colliding pair greatly extended dimer lifetimes. Thus, the onset of PAH condensation may occur for a much smaller monomer size than that which we had calculated.[3]

Extractive Sampling Studies of PAH Concentrations. Prior to the mid 1980s, there were relatively few studies in which the concentrations of individual PAH species were measured in HC flames. The most extensive data sets available at that time were those of Crittenden and Long[4] and Prado et al.,[16] which reported concentration profiles for many 2-, 3-, 4-, and 5-ring compounds and a few 6- and 7-ring molecules. Crittenden and Long[4] used quartz microprobes to sample fuel-rich premixed acetylene/oxygen and ethylene/oxygen flames at 40 Torr. Samples of stable gaseous products and the dichloromethane extract from the collected soot were analyzed by mass spectrometry, gas chromatography, and UV absorption spectroscopy. Prado et al.[16] collected gas samples containing soot with a stainless steel water-cooled probe from turbulent diffusion benzene/air and kerosene/air flames at atmospheric pressure. The methylene chloride extract was then analyzed for dissolved PAH by gas chromatography and mass spectrometry. In addition to these investigations, Di Lorenzo et al.[17] sampled PAH from fuel rich premixed methane/oxygen flames at atmospheric pressure by using a stainless steel probe cooled to 470 K by nitrogen. Individual PAH were identified by gas chromatography and

mass spectrometry. Prado et al.[18] also studied premixed flames of toluene and heptane with oxygen enriched air. Both gaseous samples and the methylene chloride extract from collected soot were analyzed by gas chromatography and mass spectrometry. Finally, Bittner and Howard[19] used a molecular beam mass spectrometer to characterize the flame structure of benzene/oxygen/argon flames at 20 Torr. Profiles of nine PAH with 2, 3, and 4 rings were measured. For all of these early flame studies, the concentration of PAH generally decreased as the number of rings increased, and the concentration of the heavier PAH was found to grow relative to the lighter PAH as a function of time. It was found that typical values for 3- and 4-ring PAH concentrations were in the range of 1−10 ppm. No evidence existed for individual PAH with molecular weights larger than 300 Da. The total concentration of PAH in a HC flame is certainly a strong function of the fuel structure and the flame conditions, such as stoichiometry, premixed versus diffusion mixing, and laminar versus turbulent flow.[20] However, the distribution of PAH was found to be relatively insensitive to the fuel structure or to the combustion conditions.

Within the past decade, the combination of molecular beam sampling from low-pressure flames with laser ionization techniques has extended the upper size limit of sampled flame species. Like the early studies, it has been observed that the concentration of PAH drops exponentially with molecular size up to species with 20−30 carbon atoms.[21] In agreement with the early work, the concentrations of the largest molecules in this size range are on the order of 1−10 ppm. However, under some flame conditions, it has been found that the concentrations of species larger than ∼30 carbon atoms do not continue to decrease and, in fact, may increase with molecular mass, leading to a bimodal distribution. For example, Happold et al. used photoionization mass spectrometry to analyze extracted samples from a low-pressure ethylene/oxygen flame and observed a

series of peaks at molecular masses >650 Da.[22] A reasonable explanation for their results is that the species responsible for the high-mass peaks are dimers (or larger aggregates) of smaller PAH.

Optical Diagnostics for PAH. Almost as soon as rare-gas plasma lasers became available in the 1970s, combustion researchers noted a visible, broadband laser-induced fluorescence that was observed in fuel-rich premixed flames or on the rich side of the stoichiometric surface in non-premixed HC flames.[23–25] In the ensuing years, scores of papers have been written that report both visible and ultraviolet emissions and have attempted to unambiguously assign the fluorescing species.[23,26–32] This rich literature has been reviewed in two recent contributions and will only be summarized briefly below.[33,34] As noted by Smyth et al.,[33] there are numerous species that might contribute to an unstructured emission in flames. In general, these candidates must be large enough so that their density of states obscures the vibrational and rotational band structure, and they must have accessible single-photon transitions at the appropriate wavelengths. PAH species meet this size criterion and have well-known ultraviolet transitions, and both probe and optical measurements put them in the correct regions of the flames studied.

In general, the wavelength of fluorescence from PAH species increases to longer wavelengths with increasing molecular size.[34] Fluorescence signals have been observed with both ultraviolet and visible excitation. By using ultraviolet excitation, two emission maxima can be observed. Although both maxima are attributed to PAH, their profiles are different. In a methane/air non-premixed flames supported on a Wolfhard-Parker slot burner, excitation at 282 nm produced two maxima in the profile of broadband ultraviolet fluorescence.[35] One of these profiles, the emission maximum of which occurs at approximately 310 nm, follows a temperature contour with increasing height above the burner surface and closely follows the peak profile for soot particles. The other feature, which peaks near 340 nm, follows a convective streamline into cooler, richer flame regions.

In premixed flames, UV excitation has been found to excite both a UV and a visible emission depending on flame location and stoichiometry.[36–39] In the recent work of Ciajolo et al.,[38] the visible emission is only seen with high PAH loading in the flame, but these researchers argue that small aromatic molecules (<4 rings) are unlikely to be its source. Rather, their work suggests that an unidentified constituent of the condensed species collected in their flames is responsible for visible fluorescence. Several groups in the soot community have postulated that early particulate matter is composed of aromatic ring systems joined by aliphatic linkages.[38,40,41] It has been proposed that these species initially form from reactions between small aromatic radicals and parent compounds or from aromatic radical recombinations. Dynamic simulations of the growth of these species predict organic structures with 1−10 nm extents, but these species appear to have lower density than graphitic carbon,[42] and they have low intermolecular sticking probabilities with each other at flame temperatures.[43] How these molecules might be expected to contribute to visible fluorescence is not well defined.

The broadband emission attributed to PAH shows strong dependencies on temperature[33,34] and may be quenched by the presence of molecular oxygen,[34] and its emission lifetime may not be a single exponential.[34] All of these factors are consistent with a more complex photophysical explanation: the source of the induced emission is aromatic condensed phase clusters as explored below.

Aromatic Excimers. In a laser-induced fluorescence experiment for an isolated molecule, an electron is excited by absorption of one or more photons, generally from the electronic ground state to an excited state. The electron may return to the ground state by emitting a photon or through one or more non-radiative steps (e.g., quenching). In a molecular condensed phase, there is a possibility that the excited state has the excitation energy delocalized across the entire aggregate structure, leading to weak bonding between adjacent molecules forming an excimer (excited dimer). In the quantum mechanical view, bonding may be dominated by charge resonance interaction, exciton (electron−hole) resonance, or mixing of the two.[44] The spectra of aromatic excimer states have been studied extensively for several decades for aggregates in solutions,[45–49] adsorbed onto surfaces, and in microcrystals.[49–54] The fluorescence from an aromatic excimer is observed substantially red-shifted from that of the isolated molecules. In addition to the shift to lower transition energies, emissions from aromatic excimers are generally broad, featureless, and highly dependent on concentration in solutions (Supporting Information, Figure 1).[55]

For the past several years, we have explored the use of semi-empirical and density functional theory (DFT) calculations of electronic transitions for small aromatic aggregates in support of the hypothesis that PAH aggregates are the source of the visible fluorescence observed in flames.[56] In general, computations with semi-empirical force fields do a poor job of predicting intermolecular binding energies because they are not parameterized for these intermolecular electronic interactions and they predict repulsive interactions for all electronic levels, including those with plane-parallel geometries and molecular separations on the order of 3.5 Å (known to be the approximate plane-separation distance in most parallel packed aromatic systems).[57]

For more exact predictions of electronic structure, ab initio methods, specifically DFT calculations, for many atom systems, are required. These calculations reveal the complex interplay between intermolecular orientation and electronic excitation. The most stable dimers of aromatic molecules with one or two rings are those with the molecular planes anti-parallel to one another because of quadrupole repulsion between the molecules in parallel, eclipsed geometries.[58] However, excited states in the same systems rearrange themselves into plane-parallel conformation attributable to excimer formation.[59]

It has been reported that DFT techniques may also inaccurately predict intermolecular interaction energies.[60,61] The situation is improving by using time-dependent DFT techniques; semi-quantitative agreement between computed and observed excimer transition energies for benzene dimers has been reported with predicted binding energies within 10% of the widely accepted experimental value (see Results and Discussion below).[62] Furthermore, several groups are now pursuing two distinct approaches to correcting binding energies either by including a damped dispersive correction to the Hamiltonian solved by the DFT routine[63,64] or by simply using the partial atomic charges resulting from the DFT calculations in a classical atom pair calculation.[65] The interaction of two molecules at medium- and long-range separation is a difficult problem that increases dramatically in complexity with molecular size. The construction of a complete potential energy surface and integration of a function which includes this surface over all space (as is required in the calculation of the equilibrium constant for dimerization from the second virial coefficient[14]) can be an overwhelming task for small PAH such as benzene molecules and prohibitively time-consuming for larger aromatic systems. Less rigorous approaches such as atom-pair models for inter-

TABLE 1: Coefficients for the Molecular Dispersion for exp-6 and Lennard-Jones 6-12 Potentials

	C−C	C−H	H−H
van de Waal[a]			
ε	0.3926	0.1435	0.0543
σ	3.475	3.208	2.937
Miller et al.[b]			
A	2376.5	523.0	114.2
B	349908	36677	11104
C	3.60	3.67	3.74

[a] Reference 58. [b] Reference 67.

TABLE 2: Values Used in Charge Set Analysis Calculations

	charge set		
atom type	Miller et al.[a]	Rubio et al.[b]	Obolensky et al.[c]
type-A carbon	−0.123	−0.1693	−0.207
type-B carbon	0.056	−0.0421	0.129
type-C carbon	0.056	−0.0421	0.129
type-D carbon	0.003	−0.013	−0.002
type-E carbon	0.000	0.000	0.000
hydrogen	0.100	0.1969	0.148

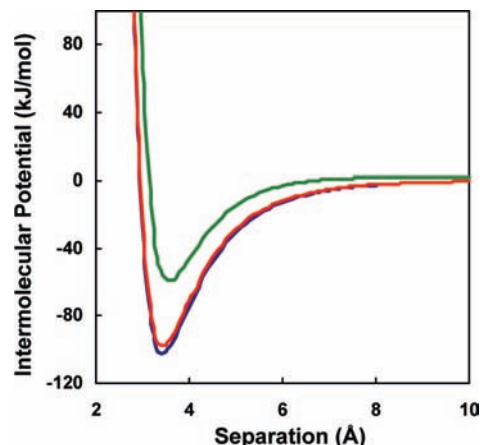[a] Reference 58. [b] Reference 83. [c] Reference 9.

Figure 2. The exp-6 formula representing dispersive forces is summed with the electrostatic formula in which one of three charge sets, listed in Table 2, is employed: Miller (blue),[58] Rubio (green),[83] and Obolensky (red),[9] in order to produce three potential energy surfaces of coronene.

molecular potentials and Monte Carlo integration in the evaluation of virial coefficients have been applied to the calculation of intermolecular interactions of large systems.

Computational Methods

The interaction potential for molecules is the sum of dispersive and electrostatic contributions. Generally, each contribution is taken as the sum of the individual interaction potential of each atom in one molecule with every atom in the other molecule. The magnitude of the atom−atom interactions is dependent on the atoms involved; it is usually derived from experimental data such as heat of sublimation data, crystal packing distances, and so forth and is evaluated from a basis set of analogous molecular species. Our group pioneered the calculation of intermolecular potentials based on atom pair interactions for large PAH aggregates more than 20 years ago.[58] Below, we evaluate atom pair parameters proposed by us in this historic context[65–68] and compare resulting interaction potentials for clusters of a series of highly condensed PAH along the Stein−Fahr stabilomer grid (Figure 1).[69]

For non-polar PAH monomers, the long-range attractive dispersive potential is dominated by instantaneous dipole-induced dipole interactions which have an r^{-6} dependence, where r is the separation between the molecules. The entire dispersive potential, including short-range repulsive contributions, have been parameterized by both Lennard-Jones potentials, such as the 6-12 potential (Table 1)[67,70–79]

$$V_{ij}^{disp} = 4\varepsilon_{ij}\left[\left(\frac{\sigma_{ij}}{r_{ij}}\right)^{12} - \left(\frac{\sigma_{ij}}{r_{ij}}\right)^{6}\right] \quad (1)$$

or, as was done in our earlier work, with an exp-6 potential (Table 1)[77–81]

$$V_{ij}^{disp} = -\frac{A_{ij}}{r_{ij}^{6}} + B_{ij}\exp(-C_{ij}r_{ij}) \quad (2)$$

The electrostatic potential between pairs of atoms on adjacent molecules is calculated from[67]

$$V_{ij}^{elec} = \left(1389.963\frac{kJ}{mol}\frac{Å}{e^2}\right)\frac{q_i q_j}{r_{ij}} \quad (3)$$

Assumptions made in establishing the effective charge on individual atoms in large PAH will have a major impact on the resulting total interaction potential. Although atom charges are available in the results of both semi-empirical and ab initio calculations, these can be highly dependent on the basis set and the methodology in calculating the atomic charge used. The charge set that we developed in our early work was based on a group-additivity scheme, which considered the local environment for each atom. As noted by Hoffman,[58,82] charge densities for hydrogen atoms in the absence of steric hindrances are

slightly positive. Carbon atoms are negatively charged if bonded to hydrogen atoms but may be slightly positive if bonded to other carbon atoms. For PAH, non-zero atomic charges are localized at the edges and approach zero for interior carbon atoms. Assumed charges for atoms in PAH are listed in Table 2. We define five types of sp^2 carbon atoms: type A, an edge carbon bonded to a hydrogen as well as two other edge carbons; type B, an edge carbon bonded to two type A carbons (e.g., the central carbons in naphthalene); type C, an edge carbon bonded to one type A and one type C (e.g., the bay carbons in phenanthrene); type D, an interior carbon bonded to one of the edge carbon types described above; and type E, a buried interior carbon bonded to only type D or type E carbons.[58,82]

To explore the dependence of intermolecular potentials on model parameters, we compared two specific dispersive parameter sets (Table 1), an exp-6 potential used in our earlier work,[58] and a Lennard-Jones 6-12 potential proposed by van de Waal[67] also in the mid 1980s, as well as three charge sets[9,58,83] (Table 2). In this and all of the computational results to follow, coordinates of planar PAH were calculated through geometry optimization by using the MM+ force field in HyperChem.[84] The resultant coordinate files were modified to include the assigned atom type and charge. Independently of the charge set used, the resultant potentials showed little dependence on the dispersive model. Potentials calculated by using a charge set proposed by Obolensky[9] agreed well with those calculated by using our 1984 charge set, despite the fact that both the hydrogen and type A carbon charges were larger in the former (Figure 2). A charge set proposed by Rubio[83] predicted lower binding energy. The most notable difference between this and the other two charge sets was a non-zero charge for type D carbons.
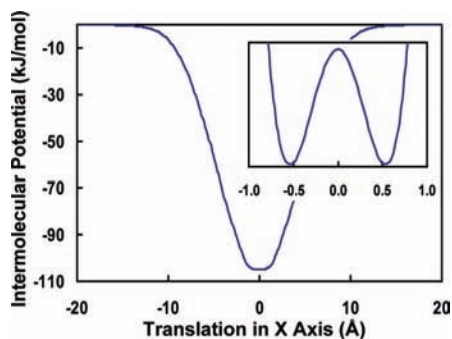
Figure 3. The intermolecular potential was calculated (by using the dispersive, electrostatic, and charge sets of Miller)[58] between two coronene molecules separated in the *z* axis by 3.5 Å. The two molecules began 20 Å apart, and while one was held constant, the other slid over it at incremental steps of 0.1 Å. The inset is a high-resolution view of the area 1 Å to either side of the completely eclipsed dimer conformation.

For dimers, binding energy minimization was accomplished by using a Simplex algorithm coded into a Delphi (PASCAL)[85] computer program. In this procedure, one of the monomers was centered at the origin and constrained to the *xy* plane. The second molecule was placed in space by random rotational orientation around three internal axes (pitch, roll, and yaw) and translation of the molecule's center of mass. (The latter is conveniently done in spherical polar coordinates to constrain the minimization search by using symmetry considerations.) It is important to note that the internal molecular structure was fixed, and only the relative molecular orientation was optimized. The geometry of minimum energy and the resultant binding energy (Supporting Information) were both found to be largely invariant of the initial geometry guess.

Calculations for clusters containing three or more molecules were performed by using an analogous Simplex algorithm. The first molecule was centered at the origin and in the *xy* plane. Subsequently added molecules were quasi-randomly distributed by slightly varying relative orientation angles but distributing the molecules at 4 ± 1 Å steps along the *z* axis.

Results and Discussion

Homo-molecular dimers. For coronene pairs, the intermolecular potentials were calculated (both by using Miller et al. dispersive and electrostatic functions and by employing the charge set from the same source[58]) for translation along a slip plane, with a constant plane-separation of 3.5 Å (Figure 3). The highest binding energy of over 100 kJ/mol was observed for a nearly, but not completely, eclipsed formation. Furthermore, substantial binding energy between the two molecules was observed even when a fairly large distance displaced them. Specifically, at a center of mass separation of 4.9 Å (which corresponds to overlap of the first pair of peripheral rings), the binding energy exceeded 50 kJ/mol.

We also investigated energy barriers to rotation around the axis of symmetry in the fully eclipsed coronene dimer. At a fixed intermolecular separation of 3.5 Å, the rotation barrier was found to be slightly less than 2 kJ/mol, less than 1% of the total binding energy, and less than $k_B T$ at flame temperatures. These calculations suggest that kinetic energy resulting from collisions could be accommodated in the aggregate's internal degrees of freedom. (See Supporting Information, Figure 2).

Minimum binding energies were calculated for a series of homo-molecular dimers along the Stein–Fahr stabilomer grid.[69] For these results, the van de Waal Lennard-Jones 6-12 dispersive
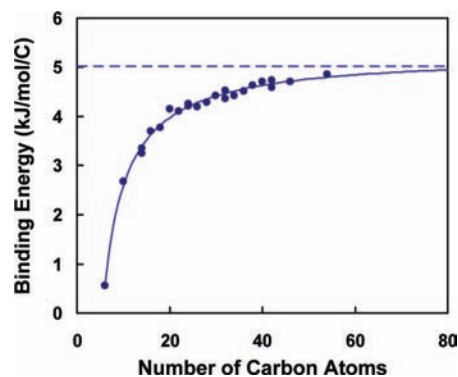

Figure 4. The binding energy per carbon atom for a series of homo-molecular dimer pairs (molecules illustrated in Figure 1). The dashed line is the experimental exfoliation energy per carbon atom in graphite.[87,90]

potential was summed with an electrostatic potential using the Miller et al.[58] charge set. For PAH less than and including coronene in size, more than 60 minimizations were performed for each dimer. On average, the binding energy varied by less than 3% with the greatest deviations observed for molecules with lower symmetry, (e.g., naphthalene and anthracene) which had two minima of similar energy (crossed and conrotated[86]). For the vast majority of dimers, the most stable configuration was the plane-parallel, displaced geometry with relatively small displacements for larger monomers. Figure 4 shows the binding energy per carbon atom in a single monomer of the homo-molecular pair, BE/*N*, plotted as a function of the number of carbons in the monomer, *N*. The data were fit to the empirical relationship

$$\frac{\text{BE}}{N} = a - \frac{b}{(N - c)} \tag{4}$$

with the best fit values for *a*, *b*, and *c* found to be 5.3 kJ/mol/C atom, 25 kJ/mol, and 0.67 carbon atoms, respectively. The value of the asymptotic limit, *a*, should be related to the exfoliation energy of graphite. Experimental values for this quantity range from as low as 35 meV/atom (from studies of the deformations of carbon nanotubes) to a high of 52 ± 5 meV/atom.[87] Despite this wide range, the majority of the recent published literature appears to favor the latter number.[60,87–89] Our value of *a* agrees with this experimental value, which is equivalent to 5.0 ± 0.5 kJ/mol/C atom.[87,90] For smaller PAH species, the difference between the calculated binding energy and this limit is a reflection of electrostatic repulsion, driven by interactions of atoms near the molecules' edges.

Hetero-molecular Dimers. In a flame, a specific aromatic molecule is unlikely to collide with an identical species. We have used the same computational approach to calculate binding energies of mixed (hetero-molecular) dimers. A total of 25 PAH ranging from benzene to circumcircumcircumcoronene ($C_{150}H_{30}$) in size were used to perform 321 unique energy minimizations, including calculations for the 23 homo-molecular dimer pairs discussed above. The binding energies for this grid of dimers are shown in Figure 5 as a surface plot. It was observed that the dimer binding energy correlated well with the reduced mass of the colliding pair (Figure 6); a result, that may be of value to the molecular growth modeling community.

It is instructive to calibrate the magnitude of PAH binding against the thermal energy of the bath gas encountered under flame conditions. Soot inception generally occurs in flames in a temperature window of 1300–1600 K. At a temperature of 1500 K, 99% of dimers with a binding energy, BE, of 57 kJ/
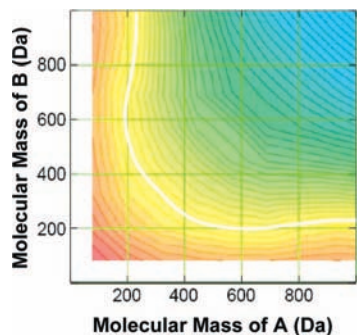
Figure 5. Surface plot of the binding energies calculated for hetero-molecular dimers. The white line represents 100 kJ/mol.
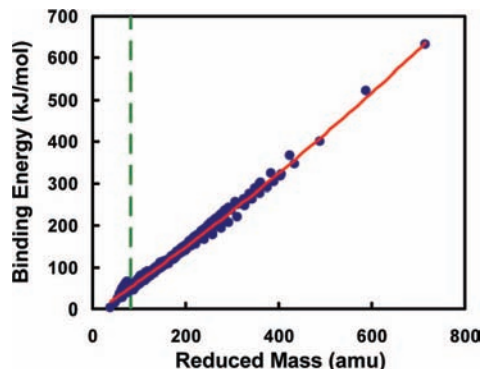

Figure 6. Calculations of binding energy for hetero-molecular dimers (blue points), trend produced (red solid line), and necessary binding energy needed for dimer survival at flame temperatures (green dashed line). Note that most of the dimers have sufficient binding energy to stay bound at flame temperatures.
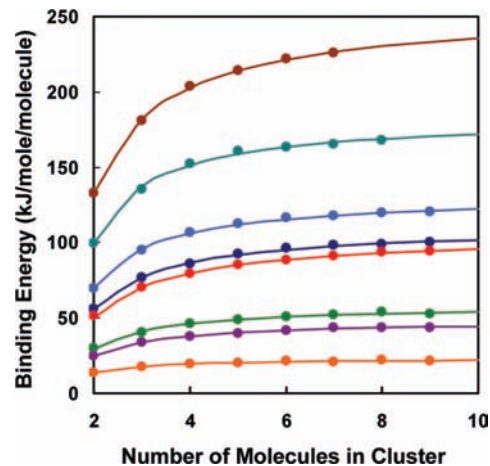

Figure 7. Binding energy (kJ/mol/number of molecules) of molecular stacks ranging from two to eight molecules. Circumcoronene (brown), hexabenzocoronene (teal), $C_{32}H_{16}$ (light blue), $C_{26}H_{14}$ (dark blue), coronene (red), pyrene (green), anthracene (purple), and naphthalene (orange) were studied.
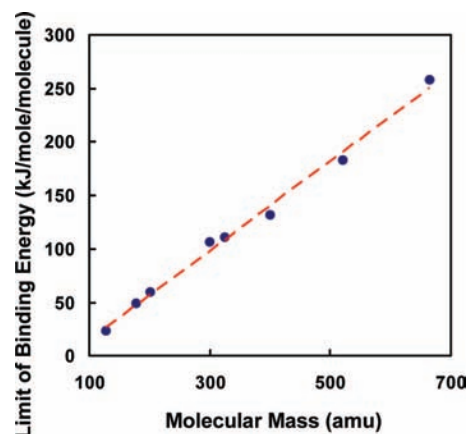

Figure 8. The limit of added binding energy per molecule of a molecular stack is linearly dependent on the size of the molecules.

mol might be expected to be stable ($e^{-BE/k_B T} \approx 0.01$). From the correlation of binding energy with reduced mass of the pair, this is equivalent to a reduced mass greater than or equal to 83 Da. The vast majority of the dimer calculations performed produce binding energies above this limit.

Homo-molecular Stacks. Calculations were performed for eight PAH molecules ranging from 128 to 666 Da in mass and arranged in stacks containing from two to nine molecules. As the number of molecules in the stack increases, the binding energy per added molecule asymptotically approaches a limit (Figure 7) that was found to depend linearly on the size of the monomer molecule (Figure 8).

The geometries of clusters of PAH have been evaluated in the context of their role in astrophysics. In 1983, van de Waal studied the geometry and stability of 13-molecule clusters of carbon dioxide, methane, benzene, cyclohexane, and naphthalene. The favorable geometry of both benzene and naphthalene was calculated to be an icosahedral (regular in the case of benzene and slightly distorted for naphthalene) structure with a single molecule in the center.[67] Rapacioli et al. studied pyrene, coronene, and circumcoronene cluster structures. For each of these, a stability threshold in the size of a single stack of molecules was observed. Their calculations suggest that clusters of pyrene arrange into multiple stacks for clusters of more than seven molecules. For coronene and circumcoronene, the transition point occurs for more than eight or seventeen molecules, respectively.[65]

Unfortunately, there are few experimental results that can be compared to these calculations. Krause et al. measured binding energies for small benzene clusters by using a two-photon, resonantly enhanced multi-photon ionization technique.[91] Binding energies of dimers, trimers, and tetramers were found to be 6.75, 26.05, and 35.70 kJ/mol, respectively. In our calculations, benzene dimers had a predicted binding energy of 3.35 kJ/mol. Fujiwara and Lim used a similar technique to determine binding energies for clusters of naphthalene, with both neutral and charged molecules. Neutral clusters of $(C_{10}H_8)_n$ where $n = 2$, 3, or 4 had binding energies of 12.06, 36.18, and 50.65 kJ/mol, respectively.[92] Calculated binding energies for the same clusters in the current work were 26.89, 53.48, and 76.85 kJ/mol, respectively. Fujiwara and Lim note that the increase in binding energy by a factor of three between trimers and dimers is explained by the fact that the trimer exists as a C_{3h} cyclic structure, as suggested by their calculations.[93] Binding energies calculated for trimers in their study were ~68 kJ/mol by using either MP2/6-31G or HFD/6-31G levels of theory. Our calculations showed a smaller relative increase in the growth of clusters $2 \rightarrow 3 \rightarrow 4$, which might be explained by the parallel-stacking geometry that we predicted.

In agreement with the astrophysics literature and observed crystal structure data, the relative importance of the electrostatic potential decreases for larger PAH and plane-parallel stacking is observed. We have compared our results for coronene clusters with those of Rapacoili et al. Our binding energies for coronene clusters, consisting of 5−9 molecules, are approximately 7% higher than those predicted in their calculations. Binding energies for clusters of larger PAH fall close to the asymptotic

Intermolecular Potential for Polynuclear HC Clusters

J. Phys. Chem. A, Vol. 112, No. 28, 2008 **6255**

trend lines predicted by our calculations. For example, their calculated binding energies of clusters of circumcoronene containing 13−19 molecules are less than 6% higher than those predicted by our trend line.[65]

Conclusions

The most critical step in the carbonization that accompanies soot inception may be the transition from two-dimensional to three-dimensional structures. In the present paper, we evaluated atom pair parameters for intermolecular interactions and compared the resulting potentials for homo-molecular dimers of several PAH along the Stein−Fahr stabilomer grid. We found that binding energies rise rapidly with molecular size and asymptotically approach the experimentally established exfoliation energy for graphite of 5.0 kJ/mol/C atom. For smaller PAH species, the difference between the calculated binding energy and this limit is a reflection of electrostatic repulsion, driven by interactions of atoms near the molecule's edge. Important empirical results have emerged from our recent calculations.

(1) The binding interaction for mixed PAH dimers correlates directly with the reduced mass of the pair.

(2) The total binding energy of PAH clusters rises with each additional molecule but approaches an asymptotic limit that depends on the molecular size.

These calculations are more rigorous than those that our group has published in the past in that more realistic potentials have been used, covering more configuration space. The new calculations suggest that binding energies for PAH are high enough that binding is thermally likely at flame temperatures for the vast majority of PAH along the Stein−Fahr stabilomer grid. Future work will include the use of these new results in an evaluation of the second virial coefficient and the resulting equilibrium constant for the condensation process. Finally, the same computational approach may be applied to binding in single and multi-walled nanotube bundles.

Supporting Information Available: Emission spectra for pyrene in cyclohexane solutions and coronene crystals. Dependence of intermolecular potential on rotation angle for eclipsed coronene dimers. Binding energies and geometric parameters for homo-molecular dimers. Image of stacks of nine coronene molecules. This material is available free of charge via the Internet at http://pubs.acs.org.

References and Notes

(1) Wagner, H. G. *Proc. Combust. Inst.* **1979**, *17*, 3.

(2) Frenklach, M.; Clary, D.; Gardiner, J., W.; Stein, S. *Twentieth Symposium (International) on Combustion*; The Combustion Institute, 1984; p 887.

(3) Frenklach, M. *Phys. Chemi. Chem. Phys.* **2002**, *4*, 2028.

(4) Crittenden, B. D.; Long, R. *Combust. Flame* **1973**, *20*, 359.

(5) Castaldi, M. J.; Marinov, N. M.; Melius, C. F.; Huang, J.; Senkan, S. M.; Pitz, W. J.; Westbrook, C. K. *Symposium (International) on Combustion*; The Combustion Institute, 1996; Vol. 26, p 693.

(6) McEnally, C. S.; Pfefferle, L. D. *Combust. Flame* **1998**, *115*, 81.

(7) Stein, S. E.; Fahr, A. *J. Phys. Chem.* **1985**, *89*, 3714.

(8) Appel, J.; Bockhorn, H.; Frenklach, M. *Combust. Flame* **2000**, *121*, 122.

(9) Obolensky, O. I.; Semenikhina, V. V.; Solov'yov, A. V.; Greiner, W. *Los Alamos National Laboratory, Preprint Archive, Physics* **2005**, 1.

(10) Donchev, A. G. *Phys. Rev. B* **2006**, *74*, 235401.

(11) Schuetz, C. A.; Frenklach, M. *Proc. Combust. Inst.* **2002**, *29*, 2307.

(12) Miller, J. H. *Proc. Combust. Inst.* **1991**, *23*, 91.

(13) Miller, J. H. *Proc. Combust. Inst.* **2005**, *30*, 1381.

(14) Miller, J. H.; Smyth, K. C.; Mallard, W. G. *Proc. Combust. Inst.* **1985**, *20*, 1139.

(15) Schuetz, C. A.; Frenklach, M. *Proc. Combust. Inst.* **2002**, *29*, 2307.

(16) Prado, G. P.; Lee, M. L.; Hites, R. A.; Hoult, D. P.; Howard, J. B. *Proc. Combust. Inst.* **1977**, *16*, 649.

(17) Di Lorenzo, A.; D'Alessio, A.; Cincotti, V.; Masi, S.; Menna, P.; Venitozzi, C. *Symposium (International) on Combustion*; The Combustion Institute, 1981; Vol. 18, p 485.

(18) Prado, G.; Westmoreland, P. R.; Andon, B. M.; Leary, J. A.; Biemann, K.; Thilly, W. G.; Longwell, J. P.; Howard, J. B. Formation of Polycyclic Aromatic Hydrocarbons in Premixed Flames. Chemical Analysis and Mutagenicity. In *Chemical Analalysis and Biolological Fate: International Symposium on Polynuclear Aromatic Hydrocarbons*; Batelle Press, 1981; Vol. 5, p 189.

(19) Bittner, J. D.; Howard, J. B. *Proc. Combust. Inst.* **1981**, *18*, 1105.

(20) Longwell, J. P. *Proc. Combust. Inst.* **1982**, *19*, 1339.

(21) Keller, A.; Kovacs, R.; Homann, K.-H. *Phys. Chem. Chem. Phys.* **2000**, 1667.

(22) Happold, J.; Grotheer, H.-H.; Aigner, M. *Rapid Commun. Mass Spectrom.* **2007**, *21*, 1247.

(23) Di Lorenzo, A.; D'Alessio, A.; Cincotti, V.; Masi, S.; Menna, P.; Venitozzi, C. *Symposium (International) on Combustio*; The Combustion Institute,1981; Vol. 18, p 485.

(24) Haynes, B. S.; Jander, H.; Wagner, H. G. *Ber. Bunsen-Ges.* **1980**, *84*, 585.

(25) Coe, D. S.; Steinfeld, J. I. *Chem. Phys. Lett.* **1980**, *76*, 485.

(26) Coe, D. S.; Haynes, B. S.; Steinfeld, J. I. *Combust. Flame* **1981**, *43*, 211.

(27) Barbella, R.; Beretta, F.; Ciajolo, A.; D'Alessio, A. *Polynucl. Aromat. Hydrocarbons: Phys. Biol. Chem., Int. Symp. 6* **1982**, 83.

(28) Miller, J. H.; Mallard, W. G.; Smyth, K. C. *Combust. Flame* **1982**, *47*, 205.

(29) Beretta, F.; Cincotti, V.; D'Alessio, A.; Menna, P. *Combust. Flame* **1985**, *61*, 211.

(30) Beretta, F.; D'Alessio, A.; D'Orsi, A.; Minutolo, P. *Combust. Sci. Technol.* **1992**, *85*, 455.

(31) D'Alessio, A.; Ciajolo, A.; D'Anna, A.; Minutolo, P. *From Mol. Dyn. Combust. Chem. Workshop Int. Inst. Pure Appl. Chem.* **1992**, 309.

(32) Ciajolo, A.; Barbella, R.; Tregrossi, A.; Bonfanti, L. *Symposium (International) on Combustion*; The Combustion Institute, 1998; Vol. 27, p 1481.

(33) Smyth, K. C.; Shaddix, C. R.; Everest, S. A. *Combust. Flame* **1997**, *111*, 185.

(34) Leipertz, A.; Ossler, F.; Alden, M. Polycyclic Aromatic Hydrocarbons and Soot Diagnostics by Optical Techniques. In *Applied Combustion Diagnostics*; Kohse-Höinghaus, K., Jeffries, J. B. Eds.; Taylor and Francis: New York, 2002; p 359.

(35) Smyth, K. C.; Miller, J. H.; Dorfman, R. C.; Mallard, W. G.; Santoro, R. J. *Combust. Flame* **1985**, *62*, 157.

(36) D'Alessio, A.; Gambi, G.; Minutolo, P.; Russo., S. *Symposium (International) on Combustion*; The Combustion Institute, 1994; Vol. 25, p 645.

(37) Ciajolo, A.; Ragucci, R.; Apicella, B.; Barbella, R.; De Joannon, M.; Tregrossi, A. *Chemosphere* **2001**, *42*, 835.

(38) Ciajolo, A.; Tregrossi, A.; Barbella, R.; Ragucci, R.; Apicella, B.; de Joannon, M. *Combust. Flame* **2001**, *125*, 1225.

(39) Minutolo, P.; Gambi, G.; D'Alessio, A.; D'Anna, A. *Combust. Sci.Technol.* **1994**, *101*, 311.

(40) Allouis, C.; Apicella, B.; Barbella, R.; Beretta, F.; Ciajolo, A.; Tregrossi, A. *Chemosphere* **2003**, *51*, 1097.

(41) Richter, H.; Benish, T. G.; Mazyar, O. A.; Green, W. H.; Howard, J. B. *Proc. Combust. Inst.* **2000**, *28*, 2609.

(42) Violi, A. *Combust. Flame* **2004**, *139*, 279.

(43) Fiedler, S. L.; Izvekov, S.; Violi, A. *Carbon* **2007**, *45*, 1786.

(44) Birks, J. B. *Photophysics of Aromatic Molecules*; Wiley-Interscience: London, 1970.

(45) Stevens, B.; Hutton, E. *Nature* **1960**, *186*, 1045.

(46) Birks, J. B.; Dyson, D. J.; Munro, I. H. *Proc. Roy. Soc. (London)* **1963**, *275*, 575.

(47) Slifkin, M. A. *Nature* **1963**, *200*, 766.

(48) Goldschmidt, C. R.; Tomkiewicz, Y.; Weinreb, A. *Spectrochimi. Acta, A: Mol. Biomol. Spectrosc.* **1969**, *25*, 1471.

(49) Seko, T.; Ogura, K.; Kawakami, Y.; Sugino, H.; Toyotama, H.; Tanaka, J. *Chem. Phys. Lett.* **1998**, *291*, 438.

(50) Fujii, T.; Shimizu, E. *Chem. Phys. Letters* **1987**, *137*, 448.

(51) Auweter, H.; Ramer, D.; Kunze, B.; Wolf, H. C. *Chem. Phys. Lett.* **1982**, *85*, 325.

(52) Daeubler, H.; Yudson, V. I.; Reineker, P. *J. Lumin.* **1994**, *60−61*, 454.

(53) Matsui, A.; Mizuno, K.; Kobayashi, M. *J. Phys., Colloque* **1985**, 19.

(54) Nelson, K. A.; Dlott, D. D.; Fayer, M. D. *Chem. Phys. Lett.* **1979**, *64*, 88.

(55) *Spectrscopy*; Straughton, Walter Eds.; Chapman and Hall: London, 1976; Vol *3*.

(56) Miller, J. H. *Proc. Combust. Inst.* **2005**, *30*, 1381.

(57) East, A. L. L.; Lim, E. C. *J. Chem. Phys.* **2000**, *113*, 89818994.

(58) Miller, J. H.; Mallard, W. G.; Smyth, K. C. *J. Phys. Chem.* **1984**, *88*, 4963.

(59) Saigusa, H.; Morohoshi, M.; Tsuchiya, S. *J. Phys. Chem. A* **2001**, *105*, 7334.

(60) Donchev, A. G. *Phys. Rev. B* **2006**, *74*, 235401/1.

(61) Grimme, S. *J. Comput. Chem.* **2004**, *25*, 1463.

(62) Amicangelo, J. C. *J. Phys. Chem. A* **2005**, *109*, 9174.

(63) Wu, Q.; Yang, W. *J. Chem. Phys.* **2002**, *116*, 515.

(64) Grimme, S. *J. Comput. Chem.* **2006**, *27*, 1787.

(65) Rapacioli, M.; Calvo, F.; Spiegelman, F.; Joblin, C.; Wales, D. J. *J. Phys. Chem. A* **2005**, *109*, 2487.

(66) Obolensky, O. I.; Semenikhina, V. V.; Solov'yov, A. V.; Greiner, W. *Int. J. Quantum Chem.* **2007**, *107*, 1335.

(67) van de Waal, B. W. *J. Phys. Chem.* **1983**, *79*, 3948.

(68) van de Waal, B. W. *Chem. Phys. Lett.* **1986**, *123*, 69.

(69) Stein, S. E.; Fahr, A. *J. Phys. Chem.* **1985**, *89*, 3714.

(70) Mainwaring, D.; Jakubov, T.; Calvitto, L. *J. Nanopart. Res.* **2005**, *7*, 59.

(71) Rapacioli, M.; Calvo, F.; Joblin, C.; Parneix, P.; Spiegelman, F. *J. Phys. Chem. A* **2007**, *111*, 2999.

(72) Lohr, L. L.; Huben, C. H. *J. Chem. Phys.* **1993**, *99*, 6369.

(73) Paterson, Y.; Nemethy, G.; Scheraga, H. A. *J. Sol. Chem.* **1982**, *11*, 831.

(74) Ornstein, R. L.; Rein, R.; Breen, D. L.; Macelroy, R. D. *Biopolymers* **2004**, *17*, 2341.

(75) Levine, H. B.; McQuarrie, D. A. *J. Chem. Phys.* **1966**, *44*, 3500.

(76) Olsen, J. R.; Legvold, S. *J. Chem. Phys.* **1963**, *39*, 2902.

(77) Kong, C. L. *J. Chem. Phys.* **1973**, *59*, 968.

(78) Han, J.; Globus, A.; Jaffe, R.; Deardorff, G. *Nanotechnology* **1997**, *8*, 95.

(79) Chalmet, S.; Ruiz-Lopez, M. F. *Chem. Phys. Lett.* **2000**, *329*, 154.

(80) Gavezzotti, A. *Chem. Phys. Lett.* **1989**, *161*, 67.

(81) Spackman, M. A. *J. Chem. Phys.* **1986**, *85*, 6579.

(82) Hoffmann, R. *J. Chem. Phys.* **1963**, *39*, 1397.

(83) Rubio, M.; Orti, E.; Sanchez-Marin, J. *Inte. J. Quantum Chem.* **1996**, *57*, 567.

(84) HyperCube, I. *HyperChem; Release 7.5, Standard Version ed.*; HyperCube, Inc.: Gainesville, FL, 2003.

(85) *Delphi 7 Professional*, 7th ed.; Borland: Austin, TX, 2002.

(86) East, A. L. L.; Lim, E. C. *J. Chem. Phys.* **2000**, *113*, 8981.

(87) Zacharia, R.; Ulbricht, H.; Hertel, T. *Phys. Rev. B* **2004**, *69*, 155406.

(88) Grimme, S.; Muck-Lichtenfeld, C.; Jen, A. *J. Phys. Chem. C* **2007**, *111*, 11199.

(89) Dappe, Y. J.; Basanta, M. A.; Flores, F.; Ortega, J. *Phys. Rev. B* **2006**, *74*, 205434/1.

(90) Donchev, A. G. *Phys. Rev. B* **2006**, *74*, 235401.

(91) Krause, H.; Ernstberger, B.; Neusser, H. J. *Chem. Phys. Lett.* **1991**, *184*, 411.

(92) Fujiwara, T.; Lim, E. C. *J. Phys. Chem. A* **2003**, *107*, 4381.

(93) Gonzalez, C.; Lim, E. C. *J. Phys. Chem. A* **2003**, *107*, 10105.

(94) Stein, S. E.; Fahr, A. *J. Phys. Chem.* **1985**, *89*, 3714.